

Learning to Identify Semi-Visible Jets

ML4JETS 2022

Related Paper: arxiv.org/abs/2208.10062

Taylor Faucett ⁽¹⁾

Daniel Whiteson ⁽¹⁾

Shih-Chieh Hsu ⁽²⁾

⁽¹⁾ UC Irvine ⁽²⁾ U Washington



Taylor Faucett



Daniel Whiteson



Shih-Chieh Hsu

A Quick Overview of Interpretability and Jet Substructure

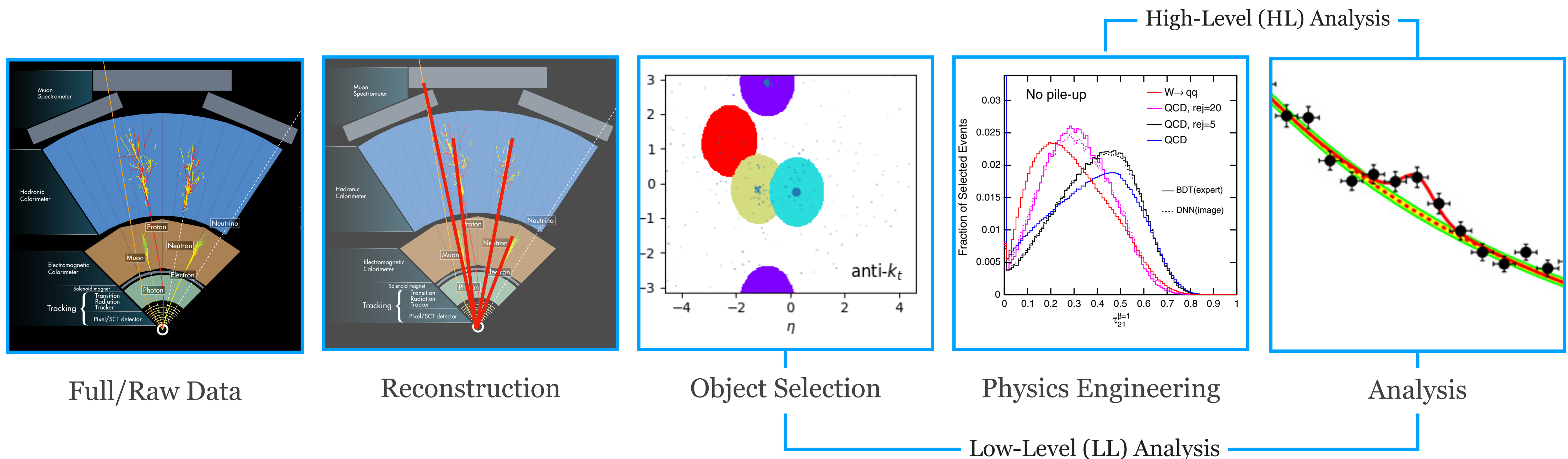
Data goes through a processing pipeline:

1. Raw Data
2. Reconstruction
3. Object Selection
4. "Physics Engineering"
5. Analysis

This has a few benefits

1. Features are physical/intelligible
2. Features are inspectable and can be validated
3. Performance Improves!

Dimensionality Reduction



- Jet: Collimated group of stable hadrons
- Form from “free” quarks/gluons which hadronize due to confinement
- Jets are detected as groups of particles in the calorimeter

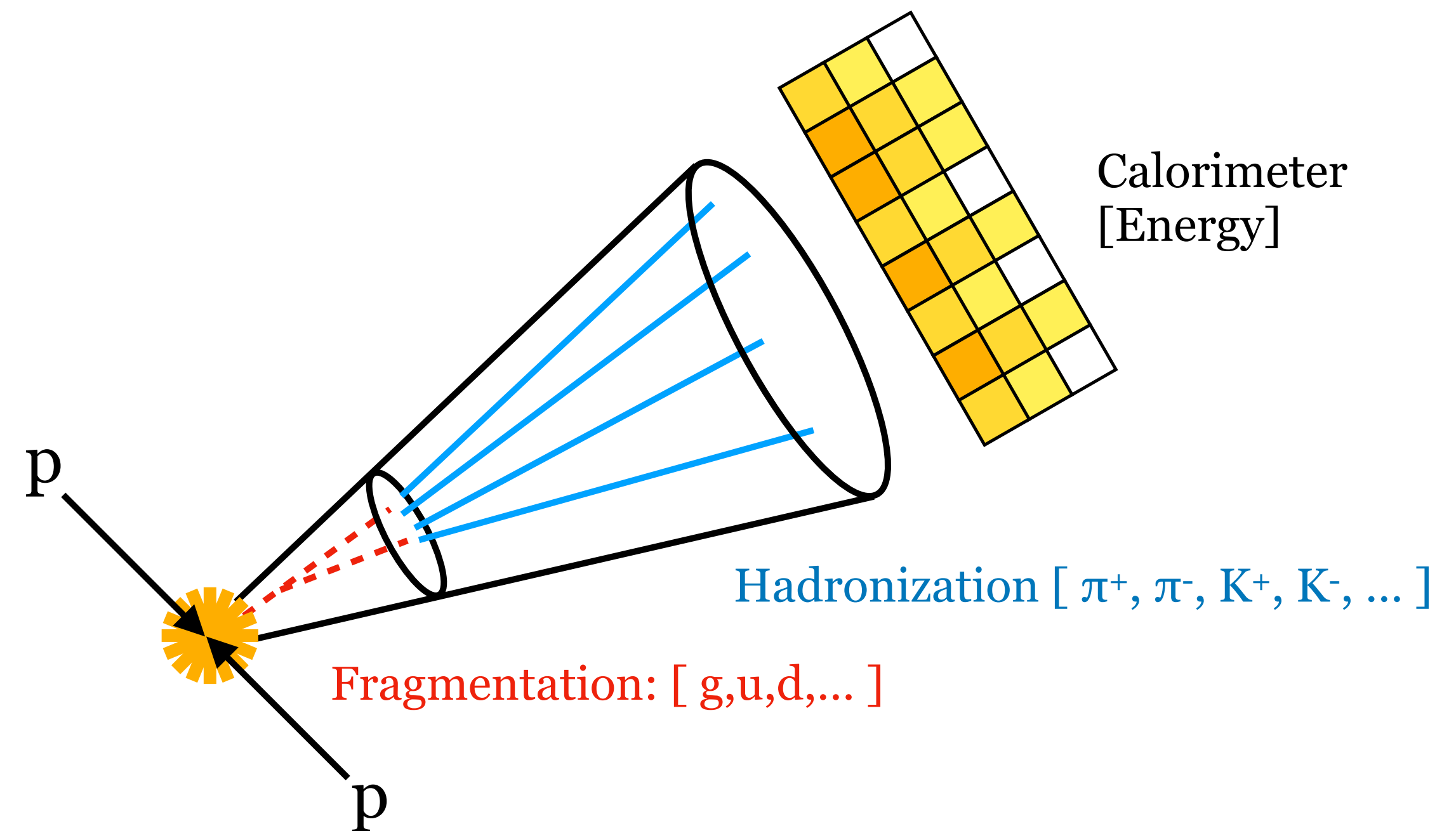
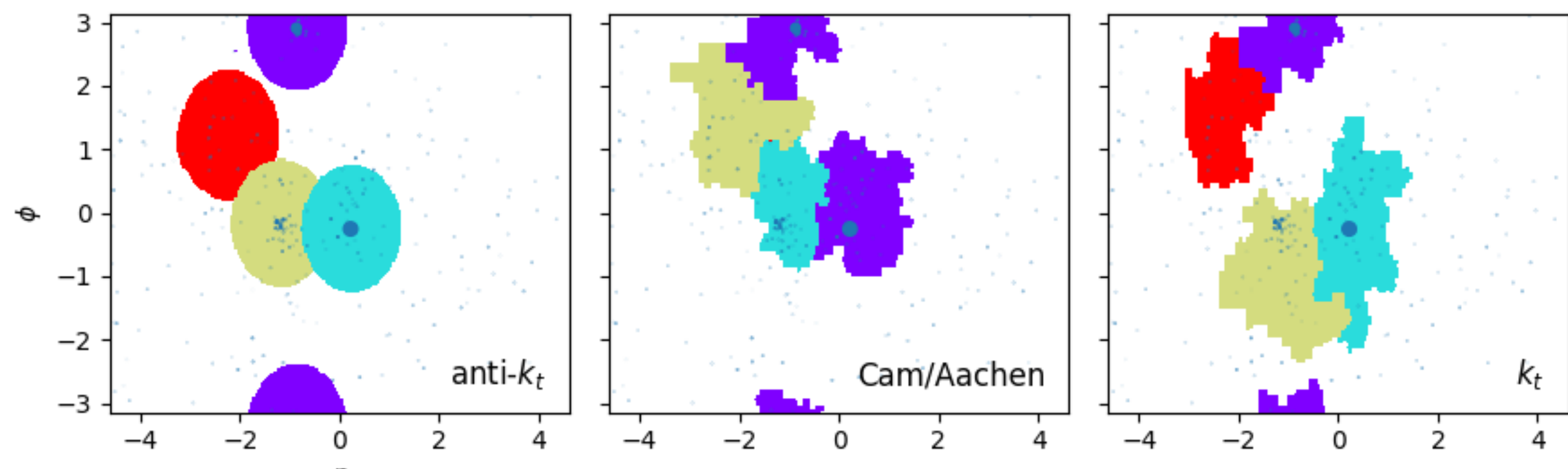


Diagram for quark/gluon hadronization



- Most Jet Substructure (JSS) observables are composed of jet constituents momentum fraction z_i and angular separation from the jet axis θ_i for a clustered jet with clustering radius R_0

$$z_i = \frac{p_{T,i}}{\sum p_T}, \quad \theta_i = \frac{R_{i,\hat{n}}}{R_0}$$

- Quark/Gluon discrimination (Generalized Angularity)

$$\lambda_\beta^\kappa = \sum_{i \in \text{jet}} z_i^\kappa \theta_i^\beta$$

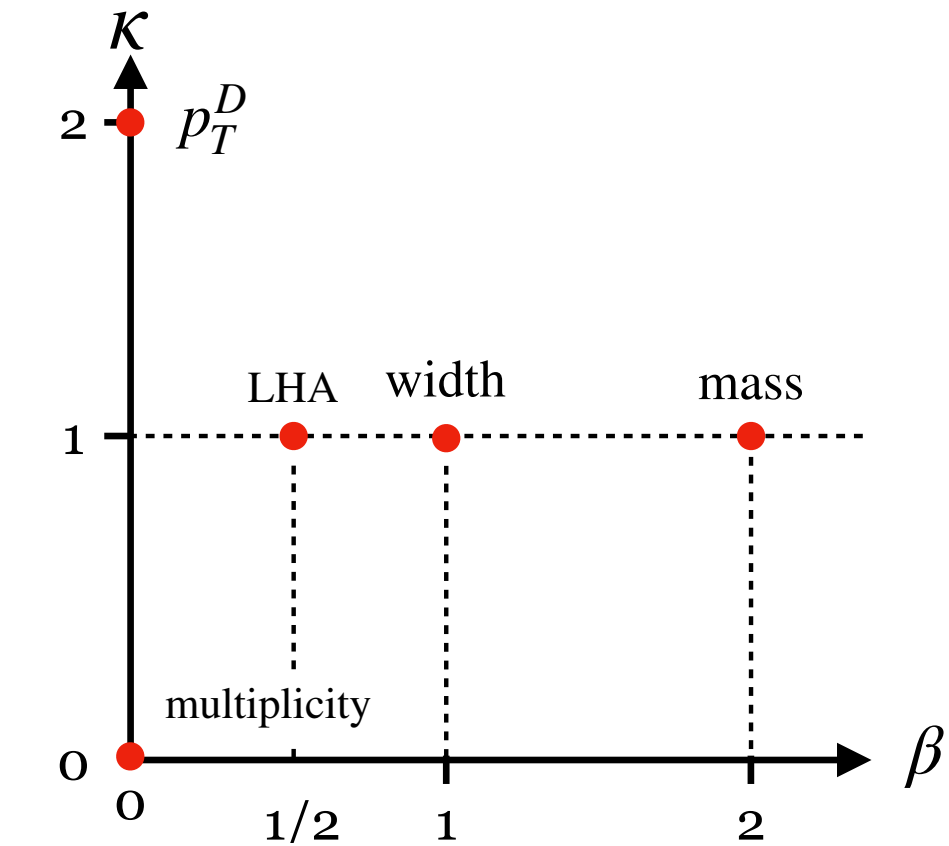
- W/Z/Higgs jets (Energy Correlation Functions = Higher Order GA)

$$ECF(2,\beta) = \sum_{i < j \in \text{jet}} p_{T,i} p_{T,j} (\theta_{ij})^\beta$$

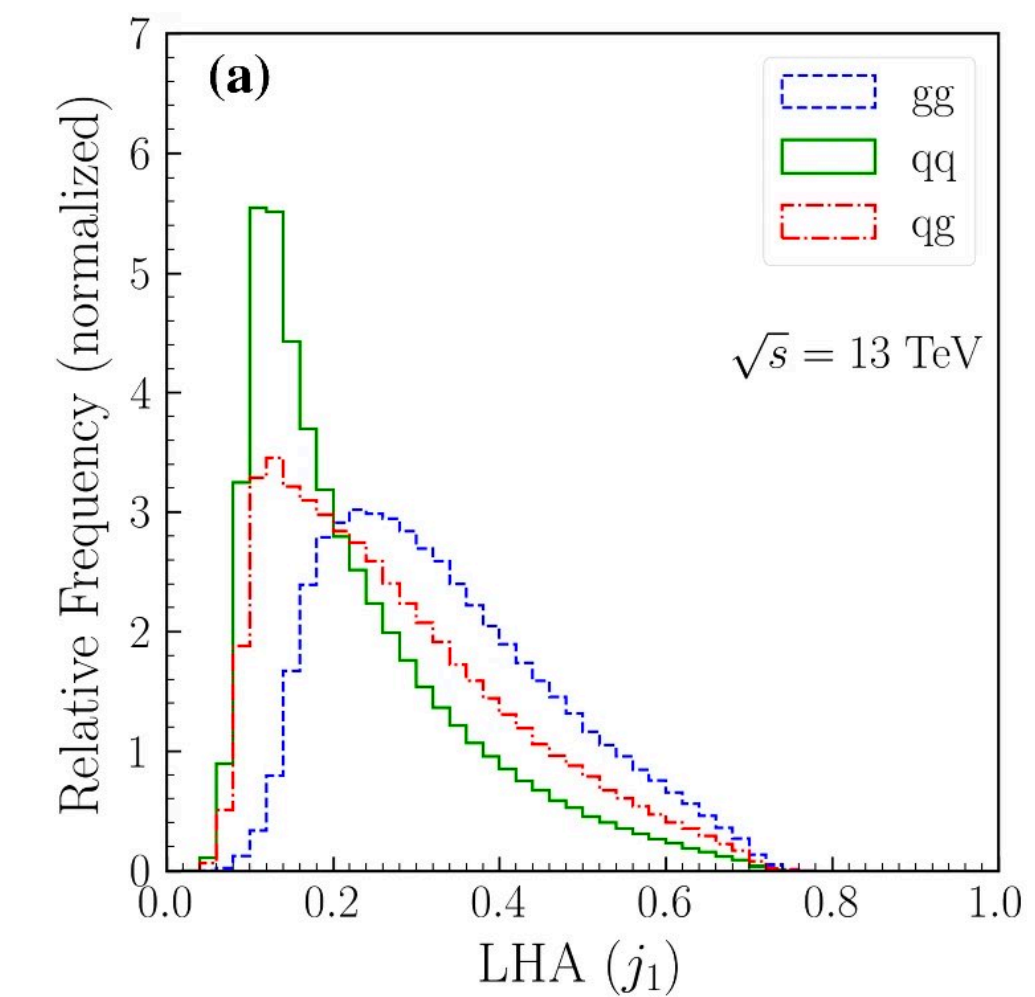
$$ECF(3,\beta) = \sum_{i < j < k \in \text{jet}} p_{T,i} p_{T,j} p_{T,k} (\theta_{ij} \theta_{jk} \theta_{ik})^\beta$$

- N-Prong sensitivity (N-subjettiness)

$$\tau_N = \frac{1}{d_0} \sum_{i \in \text{jet}} p_{T,i} \min \{ \Delta\theta_{1,i}, \dots, \Delta\theta_{N,i} \}, \text{ where } d_0 = \sum_j p_{T,j} R_0$$

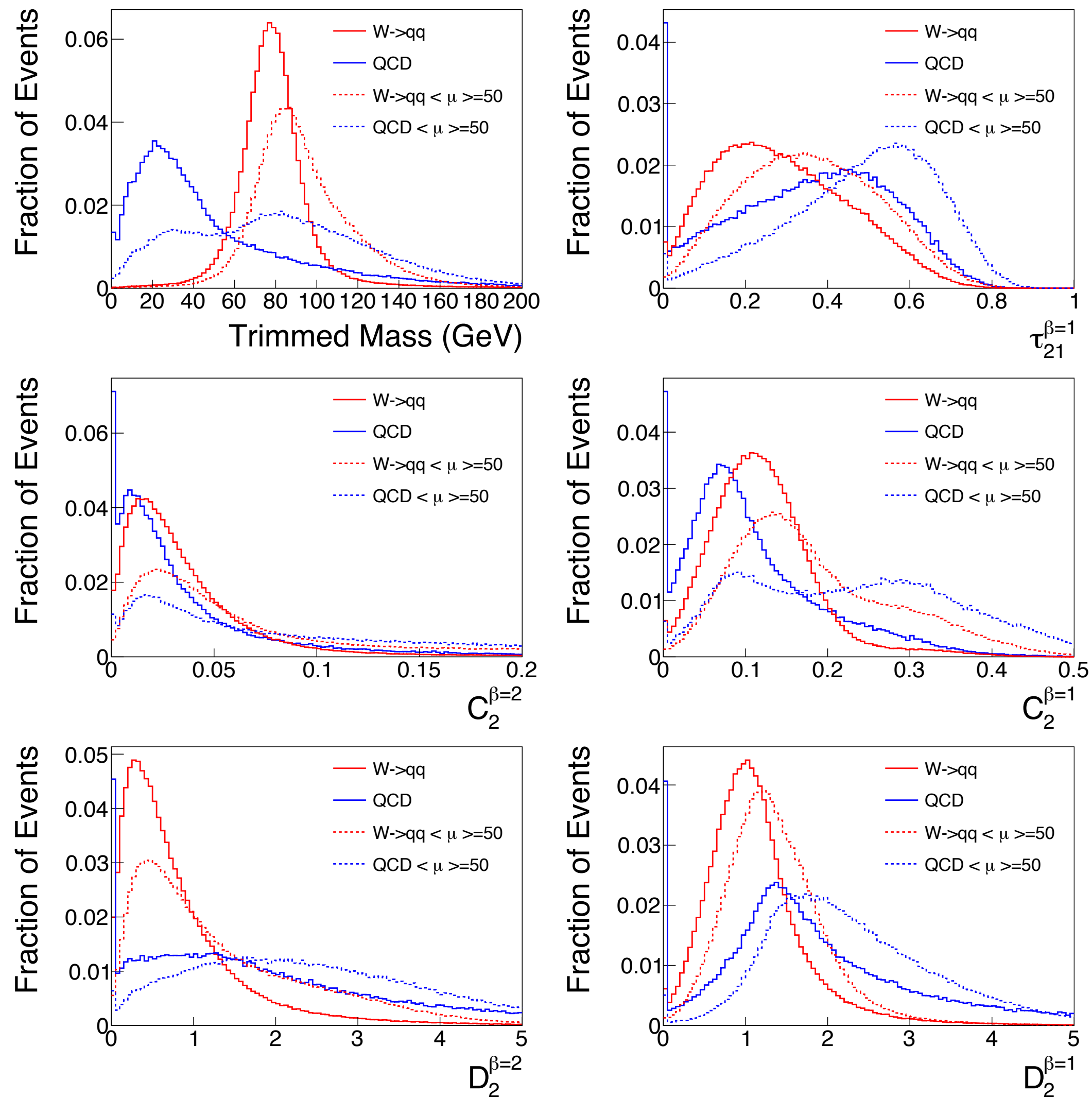


Generalized Angularity parameters



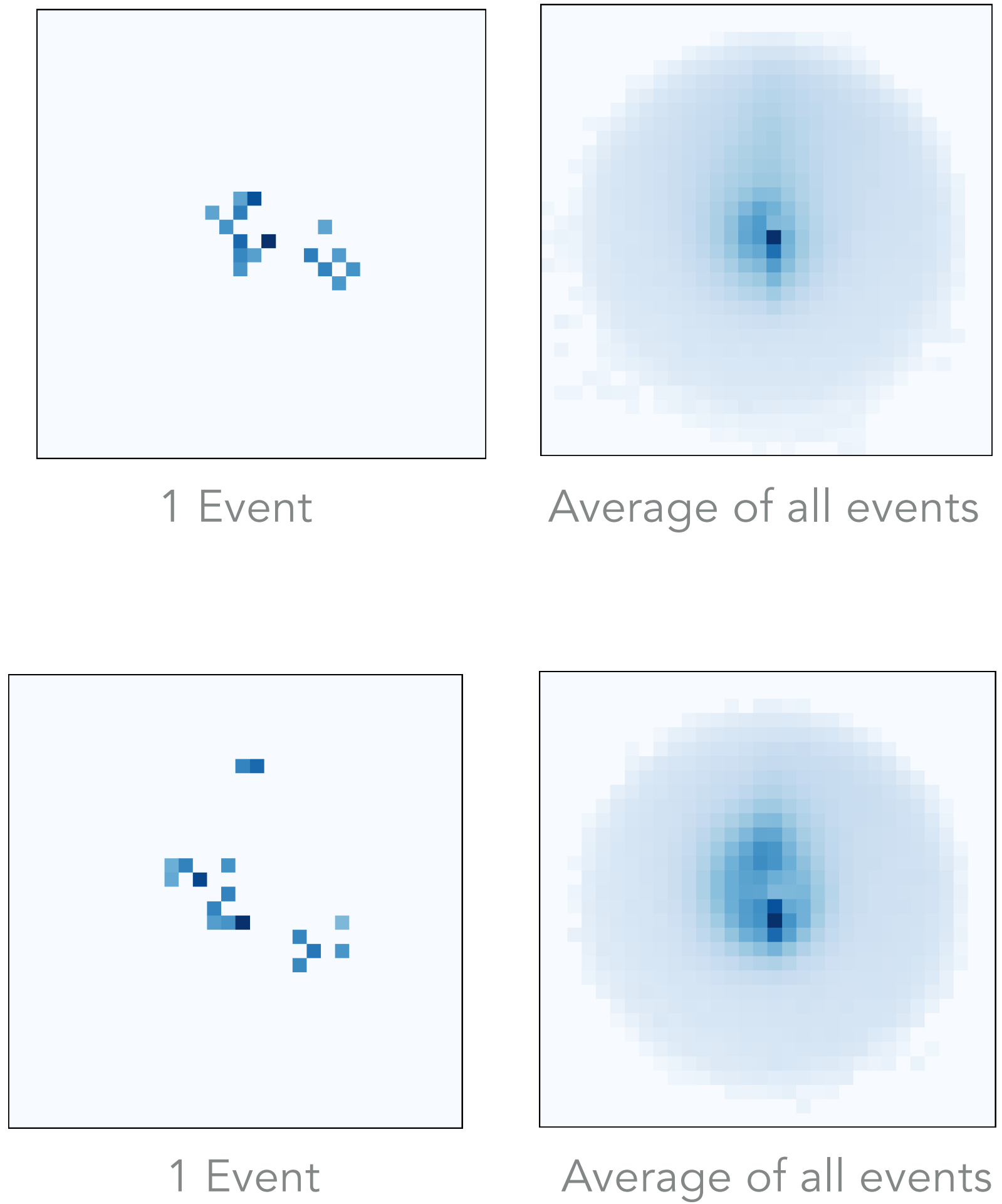
Les Houches Angularity (LHA) for quark/gluon discrimination

6 HL Variables



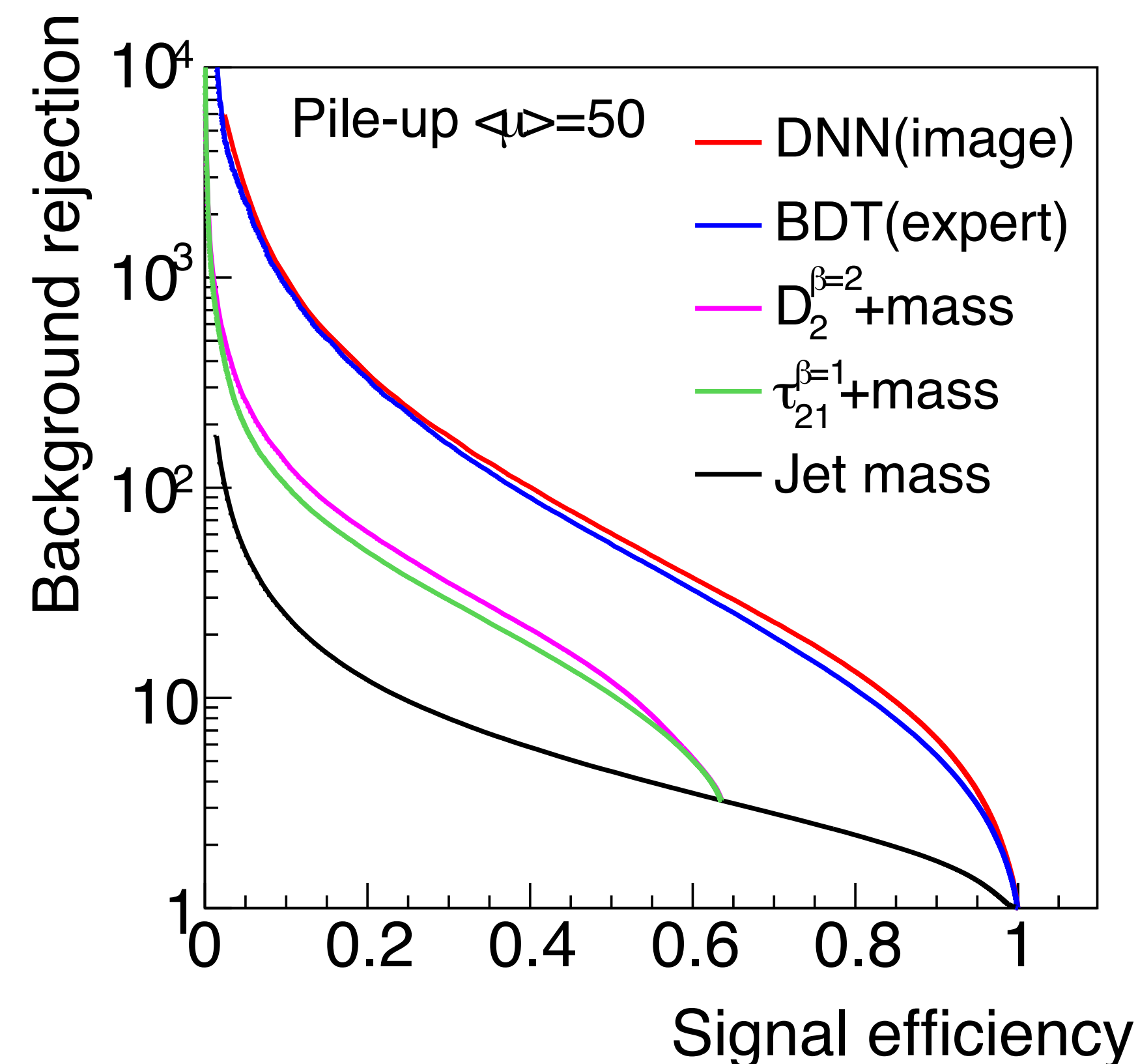
vs

LL Jet Images



- Baldi et al. find a CNN on jet images performs better than Jet Substructure
 - **Jet Images (red line):** AUC = 95.30% \pm 0.02%
 - **JSS (blue line):** AUC = 95.00% \pm 0.02%
- Where is that extra information coming from?
- Why don't our standard Jet Substructure observables contain this information?
- Is it real physics that we don't know about yet?

We've used a black box, so now what? _(ツ)_/



Baldi, P., Bauer, K., Eng, C., Sadowski, P., & Whiteson, D. (2016, March 30). Jet Substructure Classification in High-Energy Physics with Deep Neural Networks. arXiv.org. <http://doi.org/10.1103/PhysRevD.93.094034>

This is a common situation which we have proposed a solution to

- SM Jets: “Mapping Machine-Learned Physics into a Human-Readable Space”
 - <https://arxiv.org/pdf/2010.11998>
- Muon Decay Jets: “Learning to Isolate Muons”
 - <https://arxiv.org/pdf/2102.02278>
- Electron vs Jet Delineation: “Learning to Identify Electrons”
 - <https://arxiv.org/pdf/2011.01984>

Will it work for Semi-Visible jets?

- Semi-Visible Jets: “Learning to Identify Semi-Visible Jets”
 - <https://arxiv.org/pdf/2208.10062>

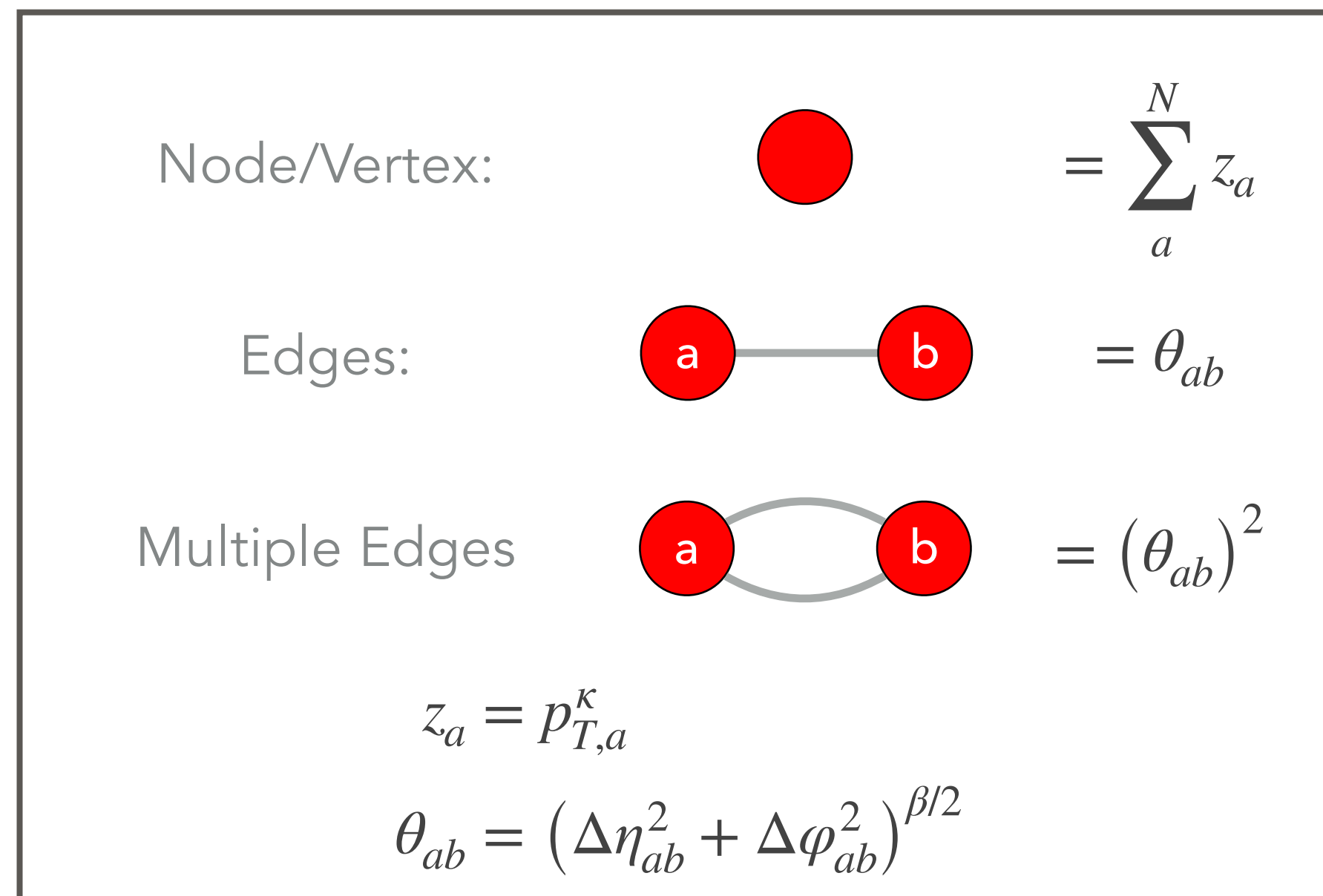
Spoiler Alert! Yes it works but with some interesting caveats unique to semi-visible jets.

Solving The Problem

Energy Flow Polynomials (EFP):
Complete linear basis set for jet substructure

The set of EFPs is defined as all isomorphic graphs, with p_T and position (θ) as defined below

Graph components

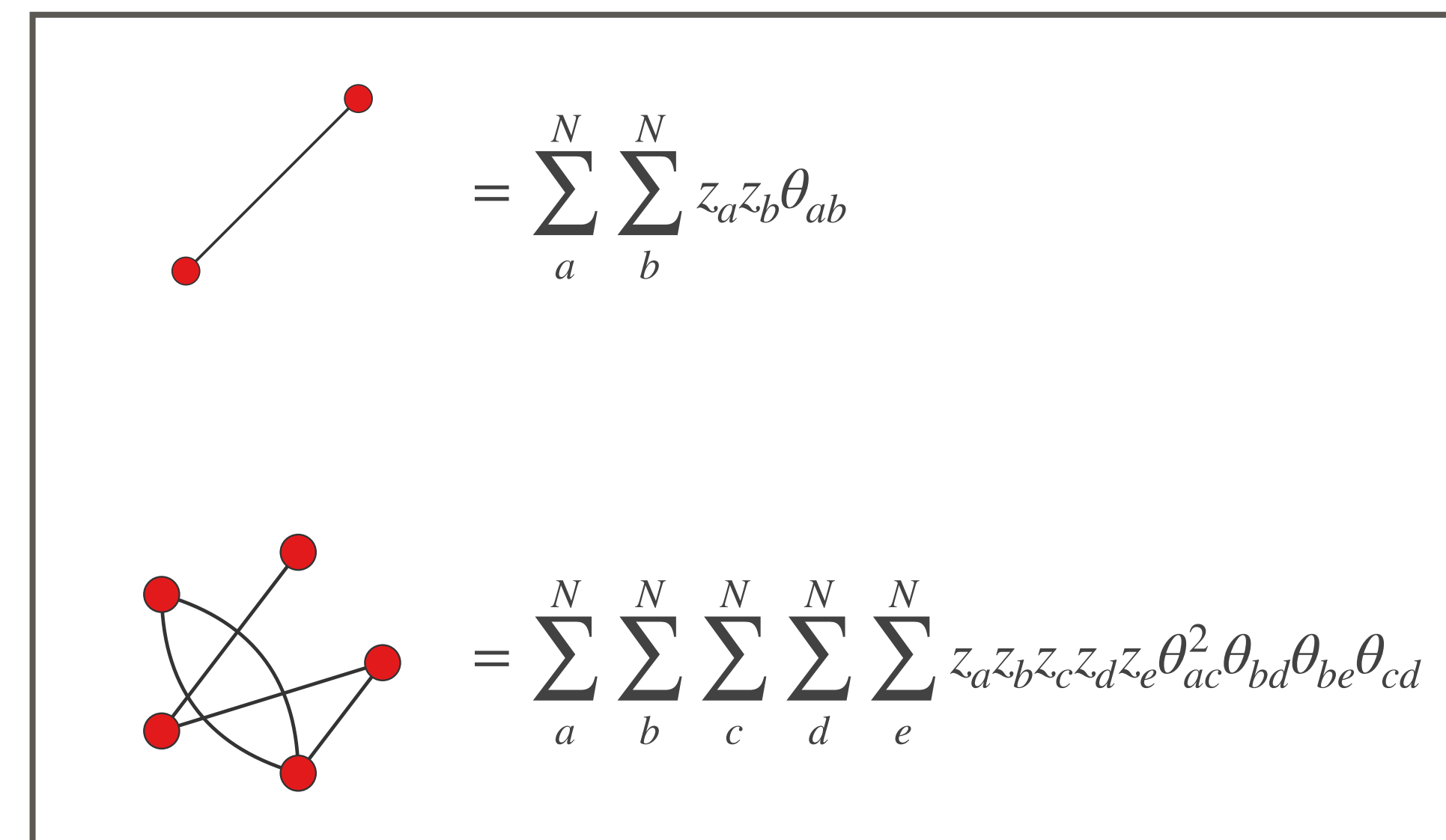


For every set of graphs, we can also modify 2 parameters (κ, β)

$$z_i = \frac{p_{T,i}^\kappa}{\sum_i p_{T,i}}$$

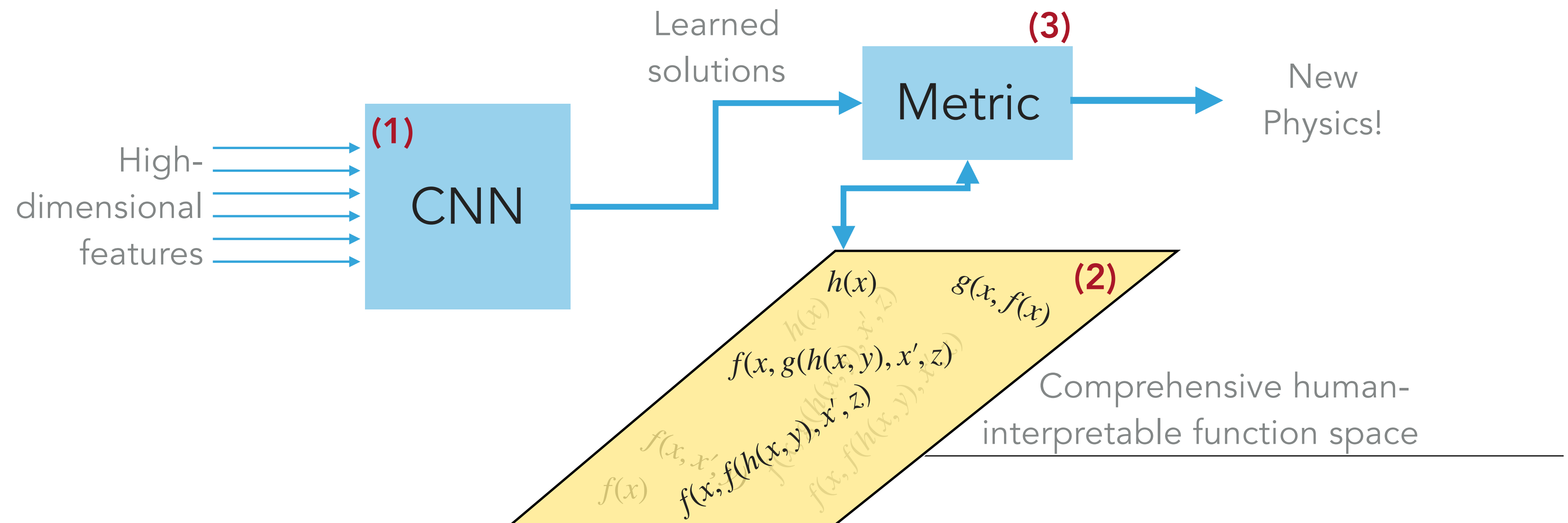
$$\theta_{ij} = (\Delta y_{ij}^2 + \Delta_{ij}^2)^{\beta/2}$$

Examples



Mapping ML to a Human Readable Space

- Can we make a model that is made up entirely of intelligible high-level features but which is “equivalent” in its decision making to the CNN? A LL solution that performs better than the HL
 - The parts we need are:
 - We have this from our CNN on jet images.
- (1) A LL but powerful solution
 - (2) A “human readable” space of HL variables.
 - (3) A metric for mapping the LL solution into the HL features.



We want an equivalent to ROC for 2 discriminating functions [f(x) and g(x)]. Classification decision of two functions at different thresholds.

Step 1

For points from signal and background (x and x'), we compare how each function maps those points relative to one another.

$$DO(x, x') = \Theta [(f(x) - f(x')) \cdot (g(x) - g(x'))]$$

Step 2

Sum over all combinations of signal/background decision orderings

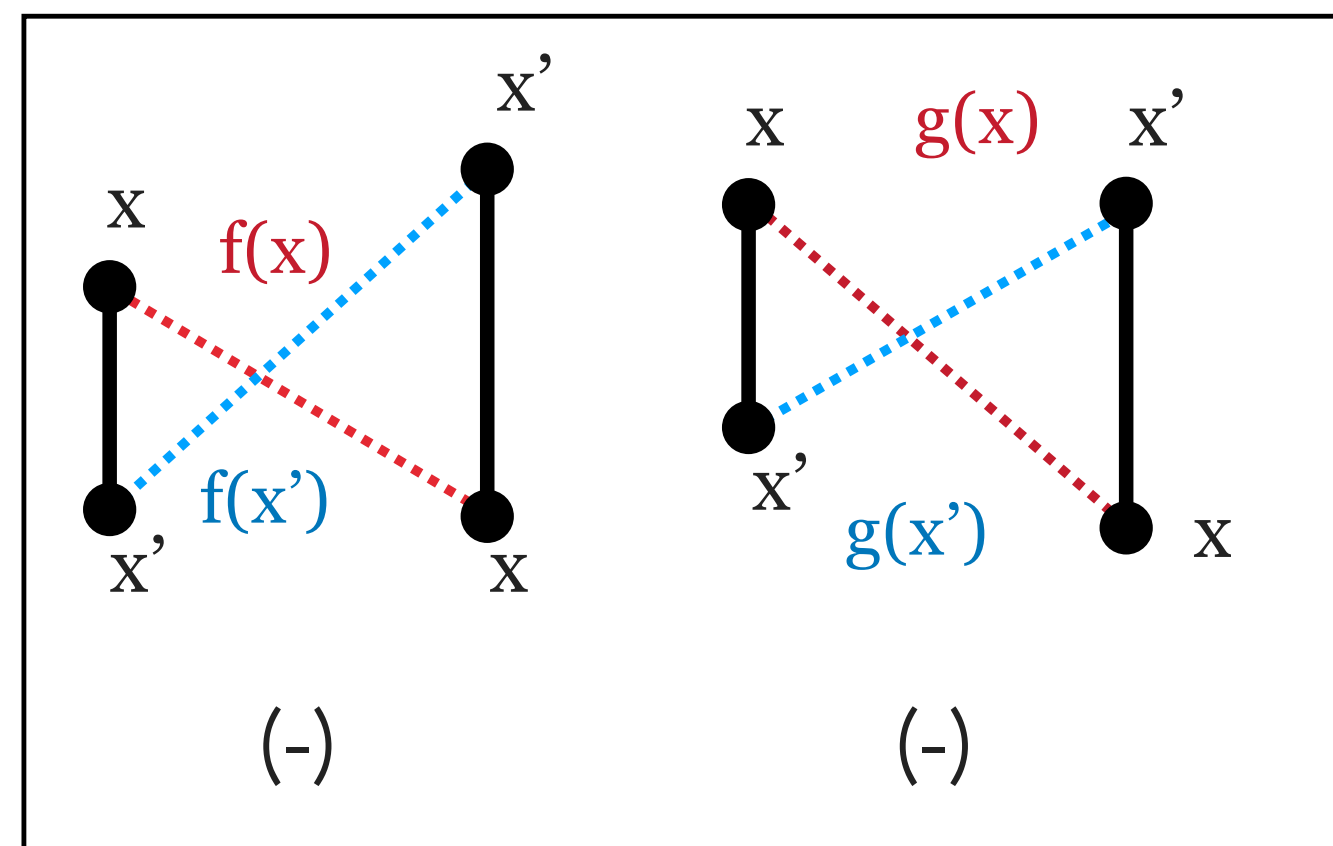
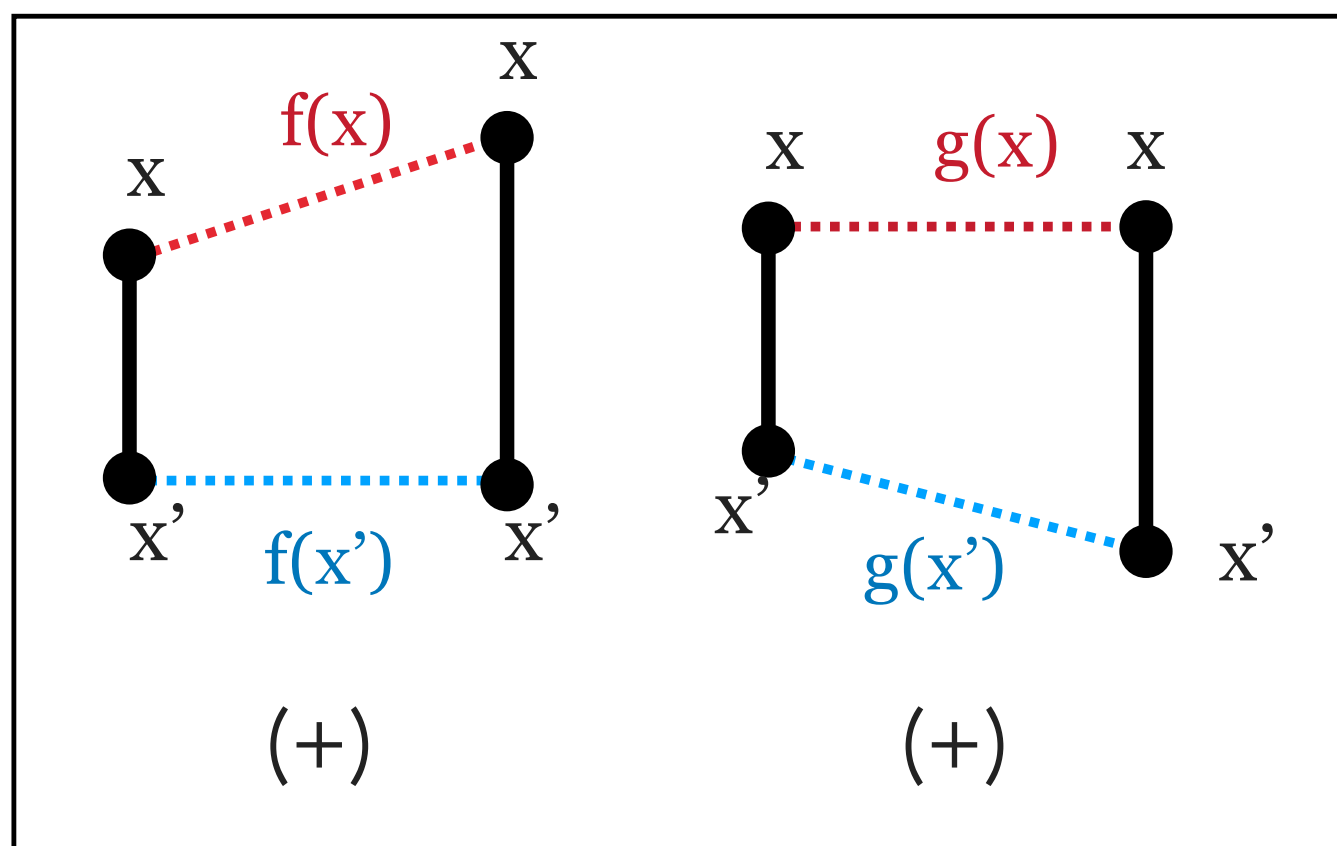
$$ADO' = \sum DO(x, x')$$

Step 3

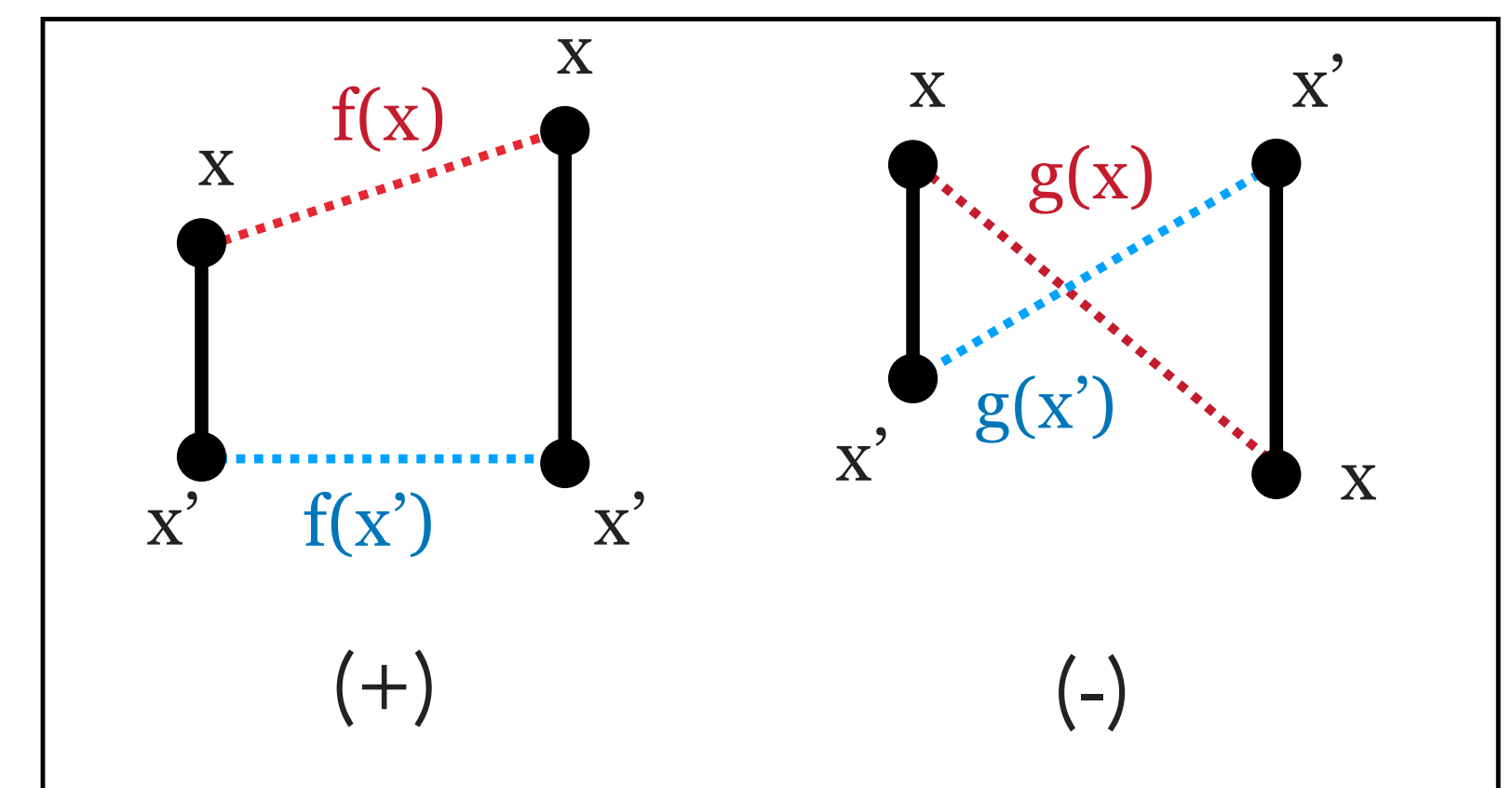
Consistent “dissimilarity” can be inverted to predict “similarity”. Map all ADO less than 0.5

$$ADO = 1 - ADO'_{< \frac{1}{2}}$$

Similar Orderings

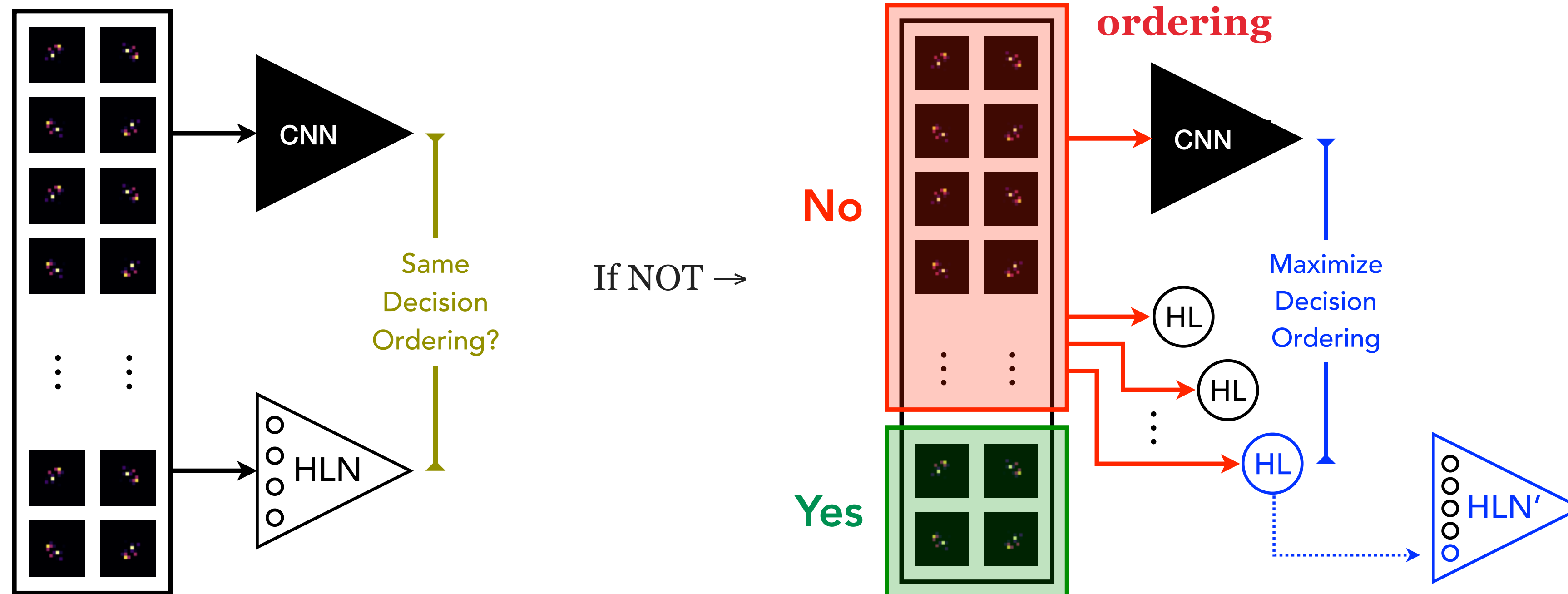


Dissimilar Ordering



We can compare NN decision making. Where does the HL network and LL network disagree?

Signal/Background Pairs



Use ADO to choose EFP that makes similar choices to the LL network in the “differently ordered” red space

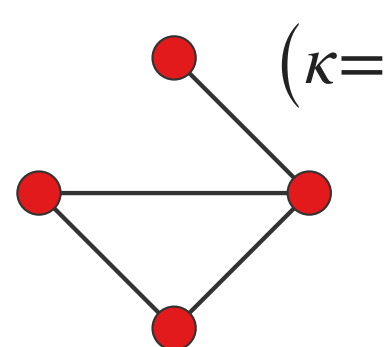
We only need 1 new observable to achieve equal performance with the CNN!

Observable	AUC	ADO[CNN, Obs.]	
M_{jet}	0.898 ± 0.004	0.807	
$C_2^{\beta=1}$	0.660 ± 0.006	0.584	
$C_2^{\beta=2}$	0.604 ± 0.007	0.548	
$D_2^{\beta=1}$	0.790 ± 0.005	0.743	
$D_2^{\beta=2}$	0.807 ± 0.005	0.762	
$\tau_2^{\beta=1}$	0.662 ± 0.006	0.600	
6HL	0.9504 ± 0.0002	0.971	Original HL
CNN	0.9531 ± 0.0002	1.000	LL network
7HL _{black-box}	0.9528 ± 0.0003	0.971	Original HL + 1 EFP

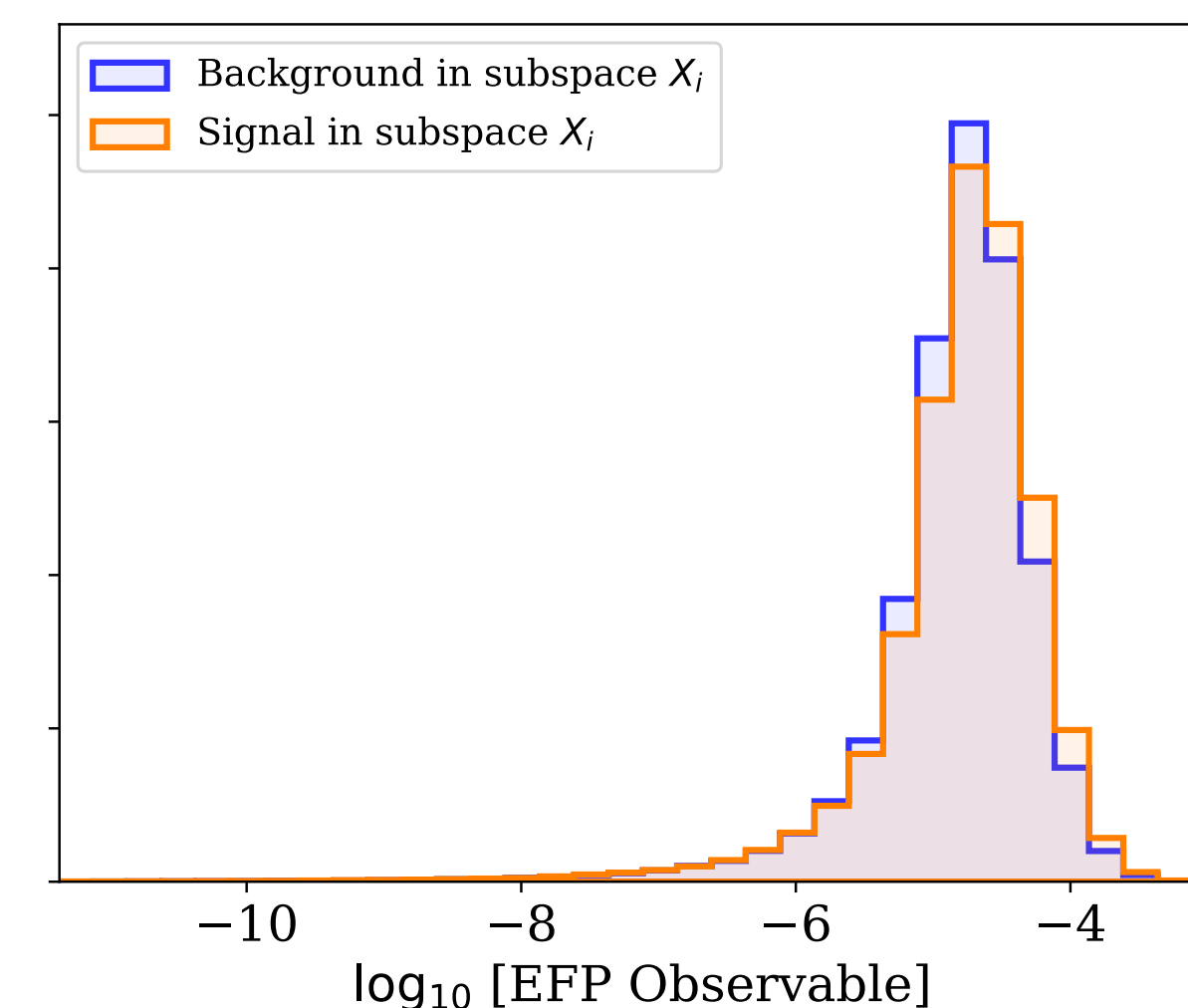
Noteworthy details about the selected EFP

- Not Infrared-safe ($k \neq 1$)
- $\beta=1/2$ is probing small-angle behaviour
- Chromatic #3 graph (probing deviations from 2-prong substructure)
- Chromatic Number = Minimum number of prongs to not vanish

Selected EFP from Guided Iteration



$$(\kappa=2, \beta=1/2) = \sum_{a,b,c,d=1}^N z_a^2 z_b^2 z_c^2 z_d^2 \sqrt{\theta_{ab} \theta_{bc} \theta_{ac} \theta_{ad}}$$



EFP Distribution (differently ordered points)

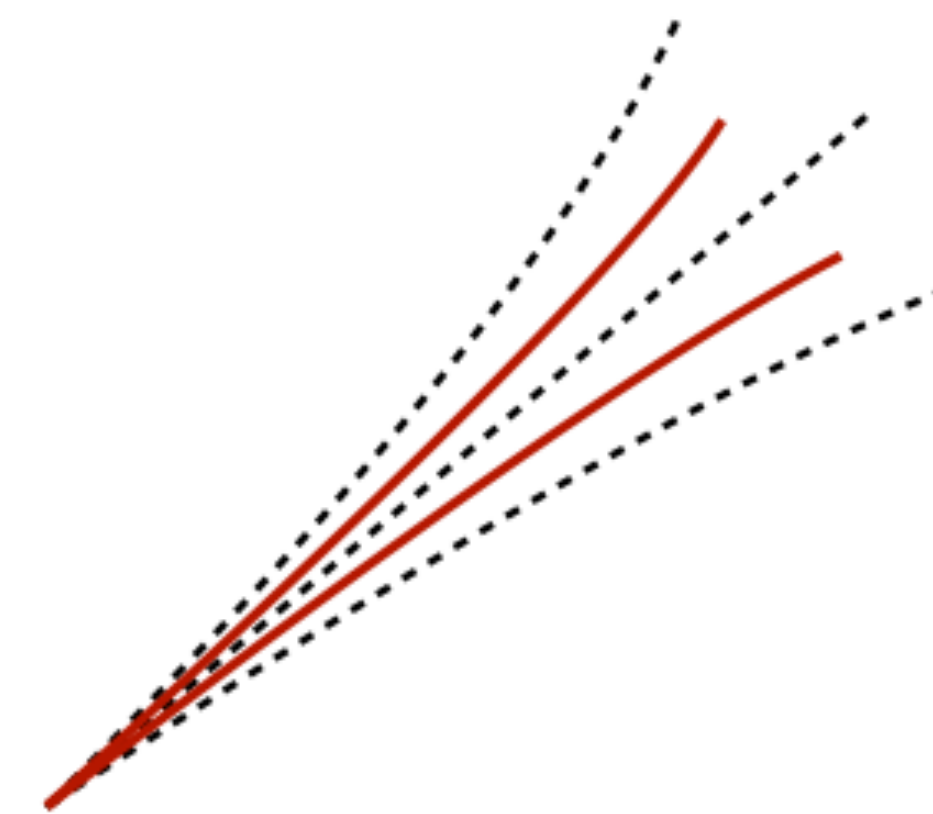
- What are Semi-Visible Jets?
 - SM process with partial decay mode into DM quarks/gluons.
 - Two popular examples described by Cohen, Lisanti, Lou (<https://arxiv.org/pdf/1503.00009.pdf>) involve an s-channel and t-channel process.
 - Decay into visible/invisible fraction is characterized by r_{inv} value

- $$r_{\text{inv}} = \left\langle \frac{\# \text{ of stable dark hadrons}}{\# \text{ of hadrons}} \right\rangle$$



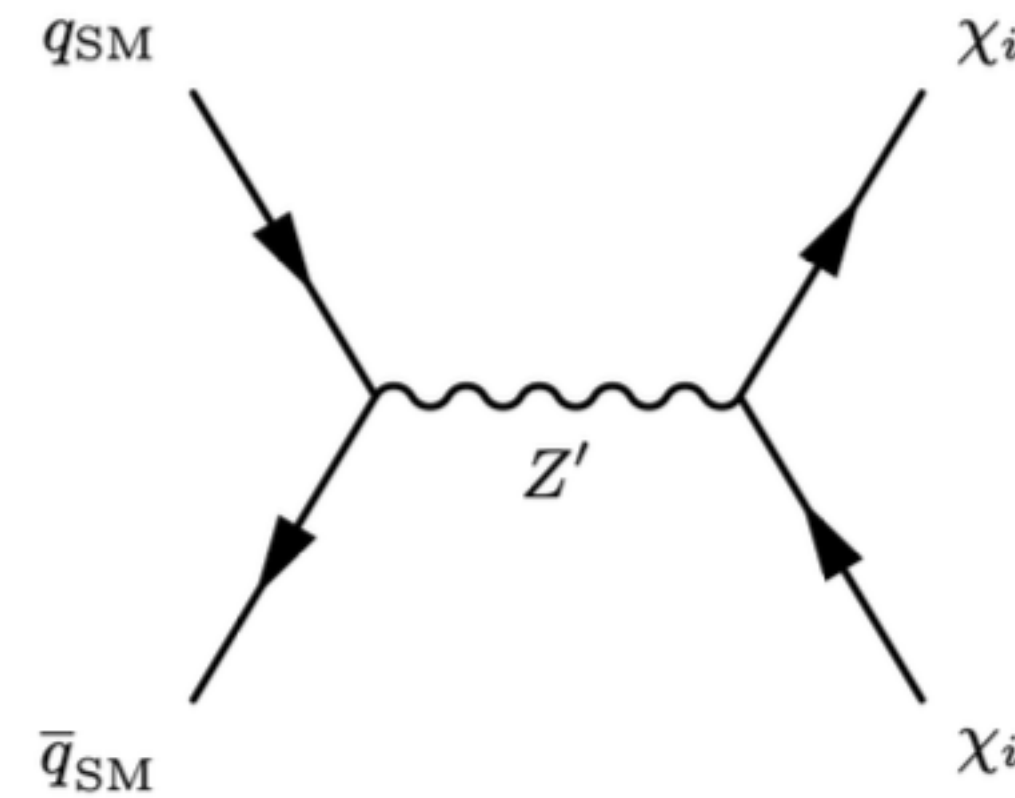
(a) Rapid Decay (Visible),
 $r_{\text{inv}} = 0$

(b) Stable Dark Jet
(Invisible), $r_{\text{inv}} = 1$

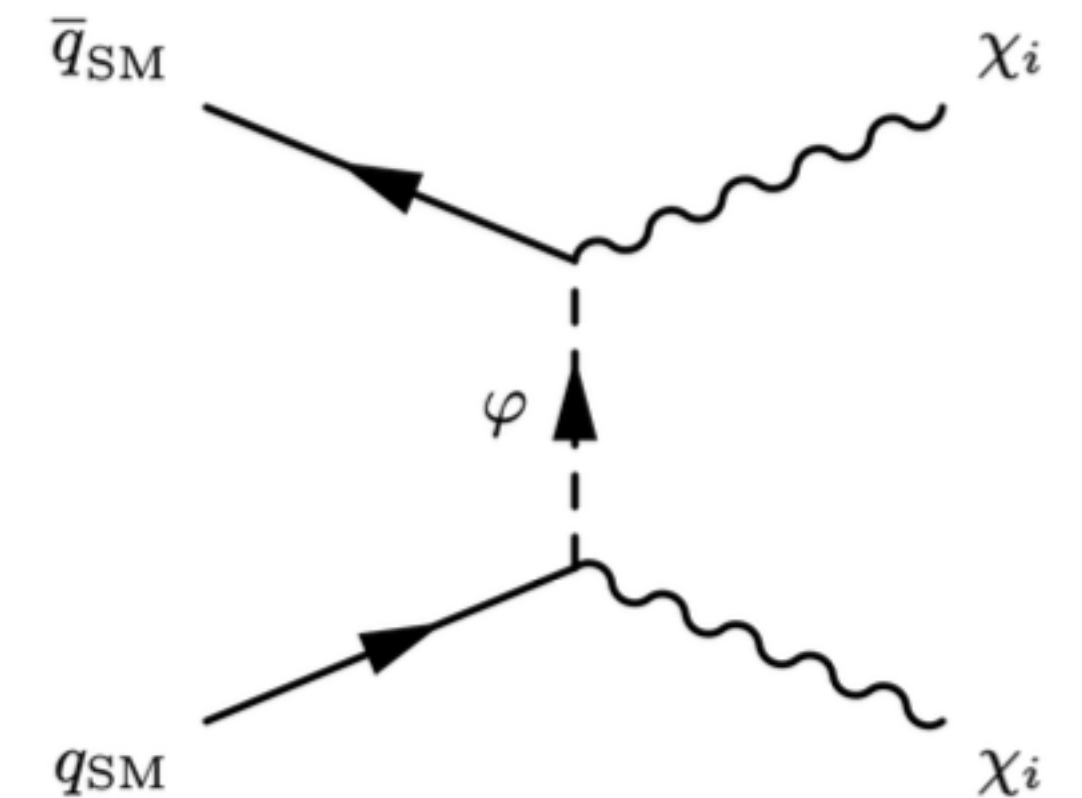


(c) Fractional Decay (Semi-Visible),
 $r_{\text{inv}} \in (0, 1)$

- Signal:
 - s-channel and t-channel SVJ
 - $pp \rightarrow Z' \rightarrow \chi_1 \bar{\chi}_1$
 - $pp \rightarrow \varphi \rightarrow \chi_1 \bar{\chi}_1$
 - COM Energy $\sqrt{s} = 13, \text{TeV}$
 - Hidden Valley settings (e.g. Mediator mass, Dark Quark mass, etc matches Cohen, Lisanti, Lou)
 - $r_{\text{inv}} = [0.0, 0.3, 0.6]$
- Background:
 - SM at the same COM energy: $pp \rightarrow jj$

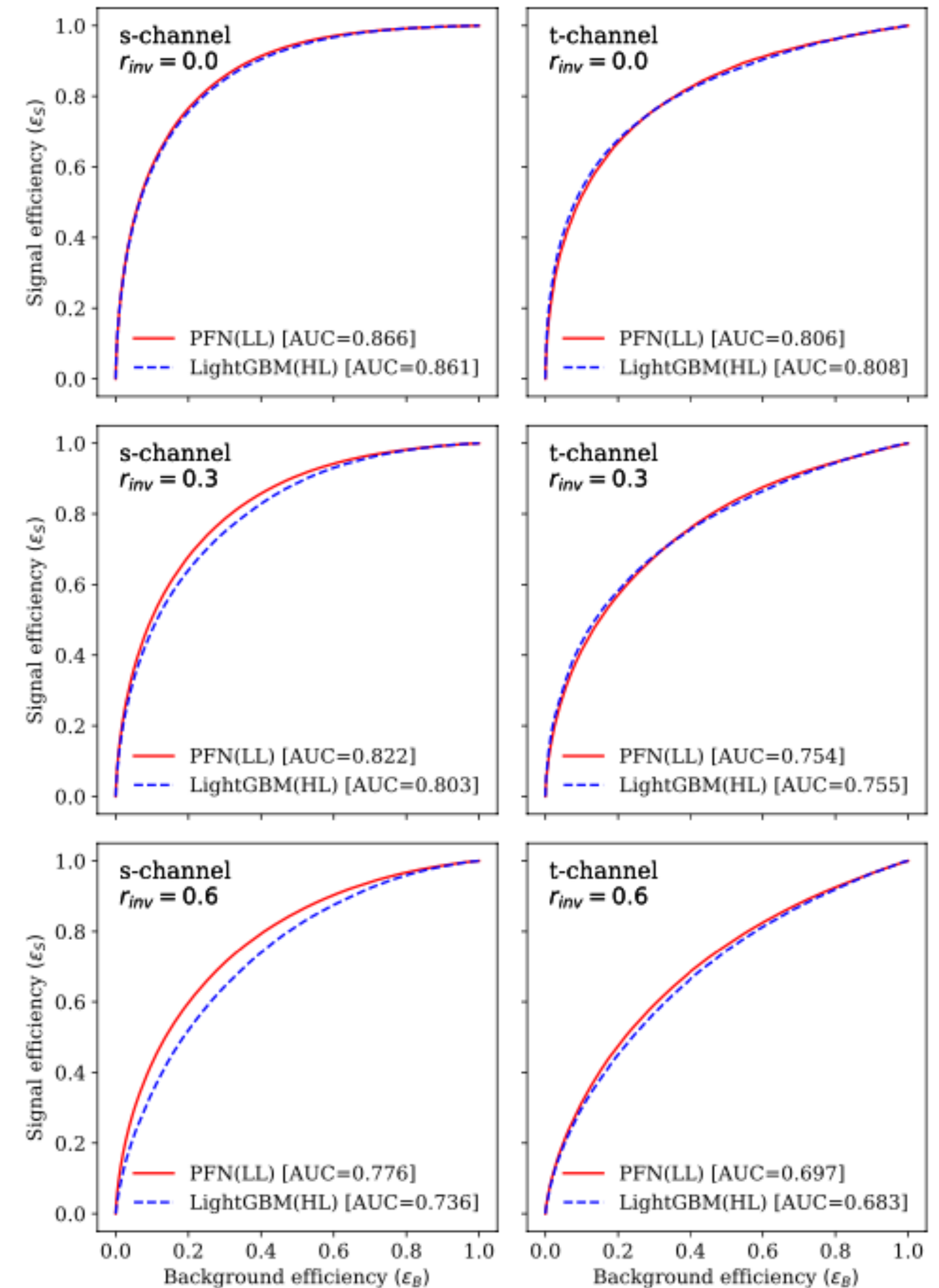


(a) s-channel







(b) t-channel

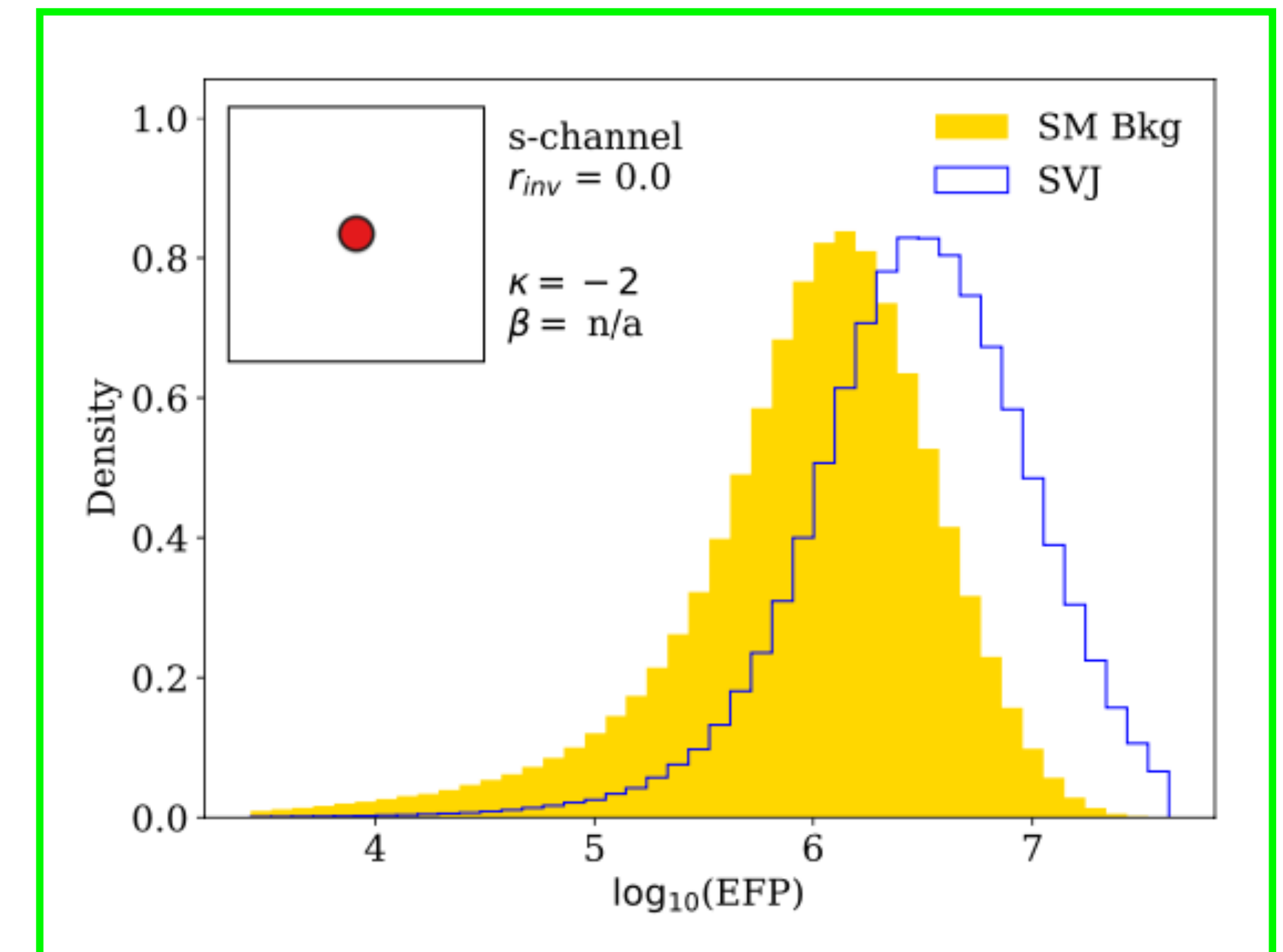
- LL trained with a Particle Flow Network using calorimeter constituents (p_T, η, ϕ)
- HL trained with a Boosted Decision Tree (LightGBM) on most common JSS features:
 - Jet p_T
 - **Generalized Angularities:** LHA, pTD, Jet width, e_{mass} , multiplicity
 - **N-subjettiness:** $\tau_{21}^{\beta=1}, \tau_{32}^{\beta=1}$
 - **Energy Correlation Functions:** $C_2^{\beta=1}, C_2^{\beta=2}, D_2^{\beta=1}, D_2^{\beta=2}, e_2, e_3$
 - **Splitting Function:** z_g











- EFP Space

- All Graphs where: $d \leq 5$, $\kappa \in [2, -1, 0, 1/2, 1, 2, 4]$ and $\beta \in [1/10, 1/2, 1, 2, 4]$

Process	r_{inv}	HL network	HL+EFP network		PFN	
		AUC, ADO[.,PFN]	EFP	κ β	AUC, ADO[.,PFN]	AUC
s-channel	0.0	0.861, 0.858		-2	0.864, 0.863	0.866
s-channel	0.3	0.803, 0.839		1 $\frac{1}{2}$	0.807, 0.840	0.822
s-channel	0.6	0.736, 0.818		-1 2	0.747, 0.821	0.776
t-channel	0.6	0.683, 0.787		-2 $\frac{1}{10}$	0.690, 0.792	0.697

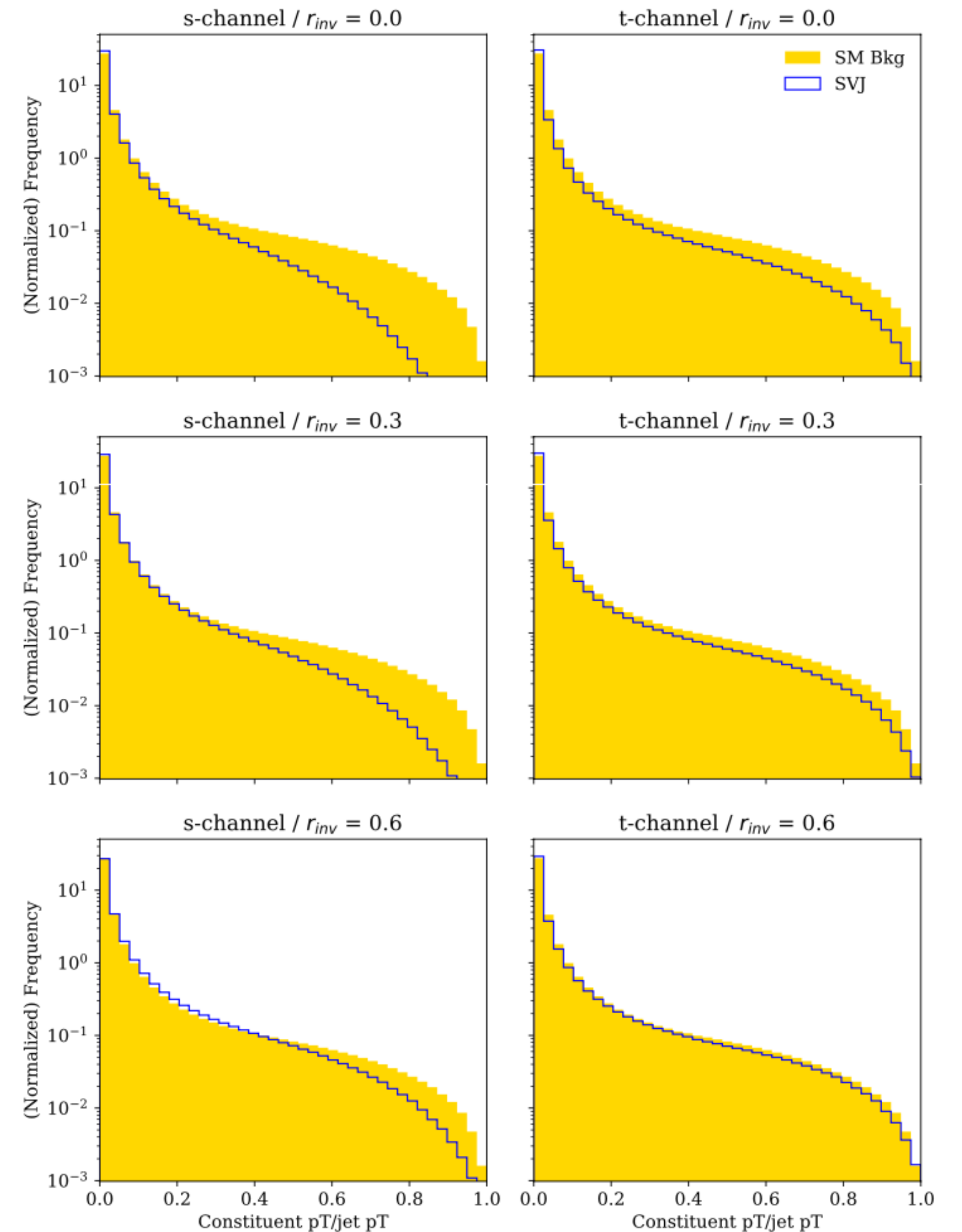


- Two potential explanations:
 - The information exists as an EFP but the guided search is failing to find it.
 - The information doesn't exist in our EFPs
- To answer this question we perform a "greedy search":
 - Train a model for every combination of HL + EFP. Do any of these combinations fill the gap?

Process	r_{inv}	HL	Pass 1			Pass 2			Guided		PFN	
		AUC	Graph	κ	β	AUC	Graph	κ	β	AUC	HL AUC	AUC
<i>s</i> -channel	0.0	0.861		$\frac{1}{2}$	2	0.864		2	$\frac{1}{10}$	0.866	0.864	0.866
<i>s</i> -channel	0.3	0.803		4	2	0.807		-1	1	0.809	0.807	0.822
<i>s</i> -channel	0.6	0.736		4	4	0.744		-2	$\frac{1}{10}$	0.747	0.747	0.776
<i>t</i> -channel	0.6	0.683		-1	$\frac{1}{10}$	0.690		-2	4	0.692	0.690	0.697

What Is Causing This?

- We are doing “Guided Iteration” because it should help tell us what the model is learning.
- What do the selected EFPs tell us about the model?
- $\kappa < 0$ values are popular choices. This is sensitive to low-pT information.
- Data processing (i.e. jet clustering and pT cuts) uses a cut of constituents $< 5\%$ of the leading pT.
- What if we relax that cut and/or raise it?
- How does that impact model performance?



s-channel									
f_{cut}	$r_{\text{inv}} = 0.0$			$r_{\text{inv}} = 0.3$			$r_{\text{inv}} = 0.6$		
	PFN	LightGBM	LL-HL Gap	PFN	LightGBM	LL-HL Gap	PFN	LightGBM	LL-HL Gap
0.00	0.908	0.895	0.013	0.853	0.829	0.024	0.788	0.739	0.049
0.05	0.866	0.861	0.005	0.822	0.803	0.019	0.776	0.736	0.040
0.10	0.847	0.848	-0.001	0.790	0.790	0.000	0.746	0.721	0.025
0.15	0.838	0.843	-0.005	0.784	0.785	-0.001	0.738	0.717	0.021

t-channel									
f_{cut}	$r_{\text{inv}} = 0.0$			$r_{\text{inv}} = 0.3$			$r_{\text{inv}} = 0.6$		
	PFN	LightGBM	LL-HL Gap	PFN	LightGBM	LL-HL Gap	PFN	LightGBM	LL-HL Gap
0.00	0.825	0.817	0.008	0.748	0.737	0.011	0.662	0.647	0.0015
0.05	0.806	0.808	-0.002	0.754	0.755	-0.001	0.697	0.683	0.014
0.10	0.741	0.742	-0.001	0.662	0.663	-0.001	0.595	0.597	-0.002
0.15	0.731	0.740	-0.009	0.655	0.661	-0.006	0.593	0.596	-0.003

- This model of Semi-Visible Jets are not well described by standard JSS observables.
- Unlike many other jet classification tasks, they are also not particularly well-described by a compact set of new observables in the EFP space.
- SVJ classification appears particularly sensitive to low-pt/soft-emission constituents and generally IRC unsafe observables.
- However, even after aggressive trimming of low-pT information some LL-HL gaps remain.
- Although Low-Level networks can capture this information, they do so in a way we can't currently explain or validate.
- These results strongly motivate a need to understand the low-pT dependence for SVJ events AND a better space than EFPs to search for observables that capture the remaining constituents.

Questions ?